Biointerface Research in Applied Chemistry
Platinum Open Access Journal (ISSN: 2069-5837)

Article
Volume 10, Issue 6, 2020, 6926 - 6935
https://doi.org/10.33263/BRIAC106.69266935

Study of the Electronic Properties of Graphene Oxide/(PANi/Teflon)

Rania Badry [1], Sara H. Radwan [1], Dina Ezzat [1], Hend Ezzat [2], Hanan Elhaes [1], Medhat Ibrahim [3,*]

[1] Physics Department, Faculty of Women for Arts, Science and Education, Ain Shams University, 11757 Cairo, Egypt
[2] Nano Technology Unit, Solar and Space Research Department, National Research Institute of Astronomy and Geophysics (Nano NRIAG), 11731 Helwan, Cairo, Egypt
[3] Molecular Spectroscopy and Modeling Unit, Spectroscopy Department, National Research Centre, 33 El-Bohouth St., 12622, Dokki, Giza, Egypt
* Correspondence: medahmed6@yahoo.com;

Scopus Author ID 8641587100
Received: 20.04.2020; Revised: 22.05.2020; Accepted: 24.05.2020; Published: 1.06.2020

Abstract: Graphene oxide (GO) has attracted enormous attention in the fabrication of electrochemical sensing systems as they have superior characteristics that enable them to be a perfect choice for the preparation of electrochemical devices. The usage of GO in preparation of polymer nanocomposites makes them a very promising material in electrical applications. Molecular modeling based on density functional theory (DFT) at B3LYP/6-31g(d, p) was utilized to study the interaction between the polyaniline (PANi) and Teflon composite with GO. The polymer blend model interacted with GO throughout the hydroxyl group (OH) located at the terminal and the oxygen atom in the middle of GO. Total dipole moment (TDM), HOMO-LUMO bandgap energy, and molecular electrostatic potential (MESP) are calculated for the studied structures. TDM found to be increased from 2.584 and 3.083 Debye for Go and PANi/ Teflon to 5.361, 4.208 and 5.839 for GO-Term (PANi/Teflon), GO- Mid (PANi/Teflon) and GO-Term (Teflon/PANi) respectively also band gap energy decreases to 0.347, 0.270 and 0.268 eV respectively. MESP shows that the reactivity is increased for the interaction of the polymer with GO through the oxygen atom in the middle. Obtained results confirmed that the proposed structure of GO/PANi/Teflon could be used in the fabrication of electrochemical devices.

Keywords: GO; Polymer composites; DFT, Polyaniline; Teflon.

1. Introduction

Polyaniline belongs to a family of polymers classified as conducting polymers [1]; it is characterized by high electrochemical activity; this dedicates it as successive electrode material for supercapacitor applications [2-4]. It is considered among the most promising materials working as energy storage material [5-6]. These applications are coming from the fact that the structure is controllable; also, it has some advantages such as low cost and environmental stability. Some researchers were reporting that the capacitive behavior in polyaniline could be attributed to the reversible electrochemical doping-dedoping process. This advantage is responsible for the phenomena of storing and further release of charge [7, 8]. For polyaniline in the electrolyte as a result of the process of oxidation/reduction leads to the process of ion transfer from solution to the polymer backbone and vice versa [9, 10]. It is reported that as far as carbon nanomaterials such as carbon nanotubes (CNTs) interacted with

polyaniline, high electrochemical stability is achieved [11, 12]. Carbon nanomaterials, including CNTs, activated carbon, and graphene, are now promising materials according to their conductivity, physicochemical stability, good and long-life cycle [13-15]. As compared to CNTs, graphene is easily handled and easily produced. Graphene is made of single layers of carbon atoms. It could be easily produced by exfoliation and separation of the individual graphite flakes [16]. Graphene is the only allotrope of carbon in which every carbon atom is tightly bonded to its neighbors by a unique electronic cloud that raises several exceptional questions to quantum physics [17-18]. It also has flexible, transparent, strong with high surface area and electrical conductivity, all of these leads to electrochemical stability. These wonderful properties, besides high specific capacitance, are dedicating graphene for supercapacitor applications [19]. The last property meets those of polyaniline and enhances their possible blending for supercapacitors as well as energy storage purposes [20-21]. Graphene oxide (GO) is a single layer of graphite oxide that is usually produced by the chemical treatment of graphite through the oxidation process [22]. It is reported that nanocomposite, depending on GO could be applied in supercapacitors [23]. Further enhancement in the electronic properties could be achieved with blending iron-doped protonated polyaniline with graphene oxide [24].

Molecular modeling with different levels and theories is now effectively used to investigate the physical, chemical, and electronic properties of many systems especially those depend on nanomaterials [25-26]. Polymers, either synthetic and/or natural, could be studied with molecular modeling; some important parameters could be achieved, such as TDM, HOMO-LUMO bandgap energy, and MESP [27-29]. It is reported that these physical properties are reflecting the reactivity of the studied structure [30-33].

The goal of this research is to study the interactions between the polyaniline (PANi)/Teflon composite and GO. The polymer model interacted with GO throughout the hydroxyl group (OH) located at the terminal and the oxygen atom in the middle. One type of GO is studied here, which takes the shape of triangular terminated with zigzag edges (ZTRI). DFT at B3LYP/6-31g(d, p) was carried out to study the TDM, HOMO-LUMO band gap energy, and MESP for the studied structures.

2. Materials and Methods

The electronic properties of GO, together with its stability, are studied theoretically via quantum mechanics rules using DFT. The DFT is used as implemented in Gaussian 09 [34] that utilizes a basis set of Gaussian type orbital functions. The Becke-three parameters-Lee-Yang-Parr hybrid functional (B3LYP) [35-37] with basis set 6-31g(d, p) is employed in the calculations at Spectroscopy Department, National Research Centre. One type of GO is studied here, which takes the shape of triangular terminated with zigzag edges (ZTRI). One polymer system is studied, which is based on a blend of PANi/Teflon. The effect of GO presence on the physical properties of the composite system is presented in terms of TDM, bandgap energy (ΔE), and MESP.

3. Results and Discussion

3.1. Building model molecules.

Before the attachment of the studied polymer blend onto the GO surface, the polymer blend model based on PANi/ Teflon is first explored. For the model molecule representing

PANi/Teflon, one unit of Teflon is proposed to interact with four units of PANi. The model molecules representing PANi/Teflon and GO presented in figure 1.

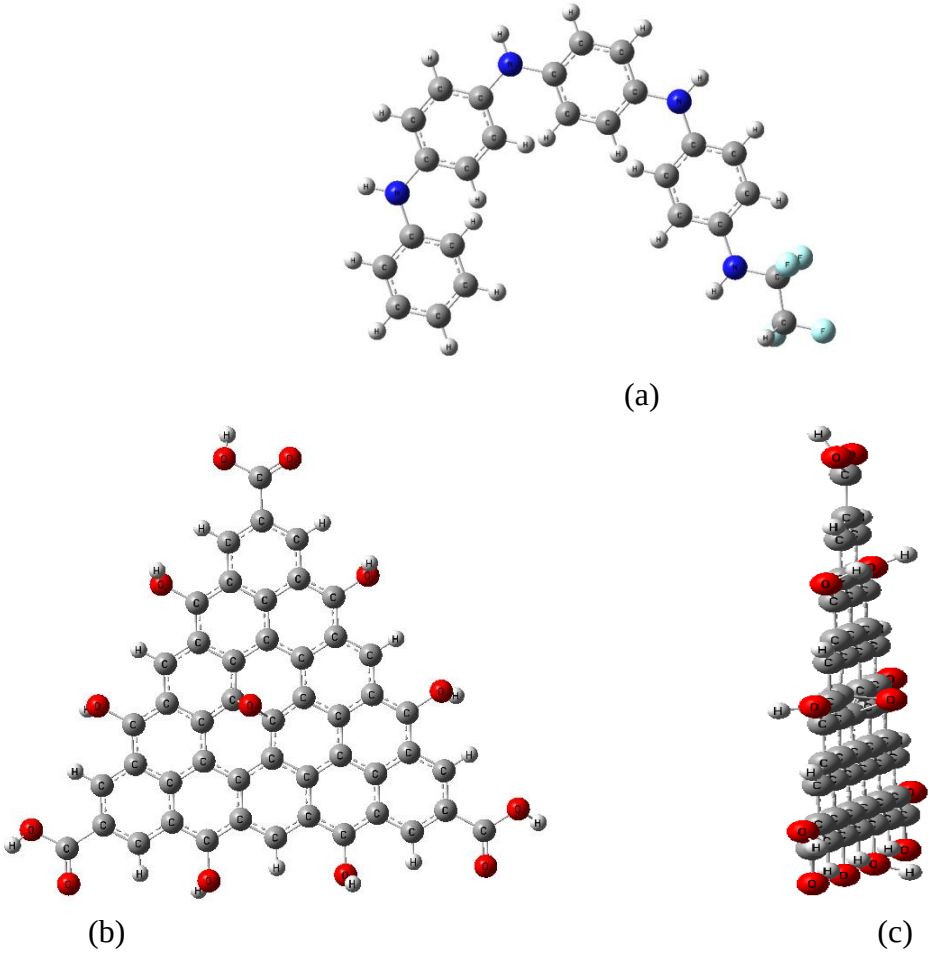

(a) (b) (c)

Figure 1. Model molecules were representing (a) fully optimized PANi/Teflon model, (b) top view of optimizing GO model, and (c) side view of optimized GO, respectively.

The interaction of the individual polymers PANi and Teflon occurred throughout the amine group of PANi. Additionally, the interaction of PANi with Teflon is supposed to be strong interaction, i.e., complex state. On the other hand, the polymer blend model could interact with GO from PANi side or Teflon side throughout the hydroxyl group (OH) located at the terminal and the oxygen atom (O) in the middle of GO structure based on the previous finding [38]. Figure 2 shows the optimized structures describing GO interacted with PANi/Teflon throughout the terminal of GO and that throughout the middle O atom of GO.

3.2. Electronic properties.

In order to follow the changes that occurred in the electronic properties of PANi/ Teflon model molecule and any other materials as a result of the chemical modifications in its structures, both TDM and band gap energy ΔE are calculated.

Table 1. The bandgap energy (ΔE) as eV and the total dipole moment (TDM) as Debye of GO, PANi/Teflo, and GO interacted with PANi/teflon model through the middle O atom of GO calculated at B3LYP/6-31g(d,p).

Structure	TDM	ΔE
GO	2.584	0.345
PANi/Teflon	3.083	1.738
GO-Term (PANi/Teflon)	5.361	0.347
GO- Mid (PANi/Teflon)	4.208	0.270
GO-Term (Teflon/PANi)	5.839	0.268
GO- Mid (Teflon/PANi)	1.436	0.301

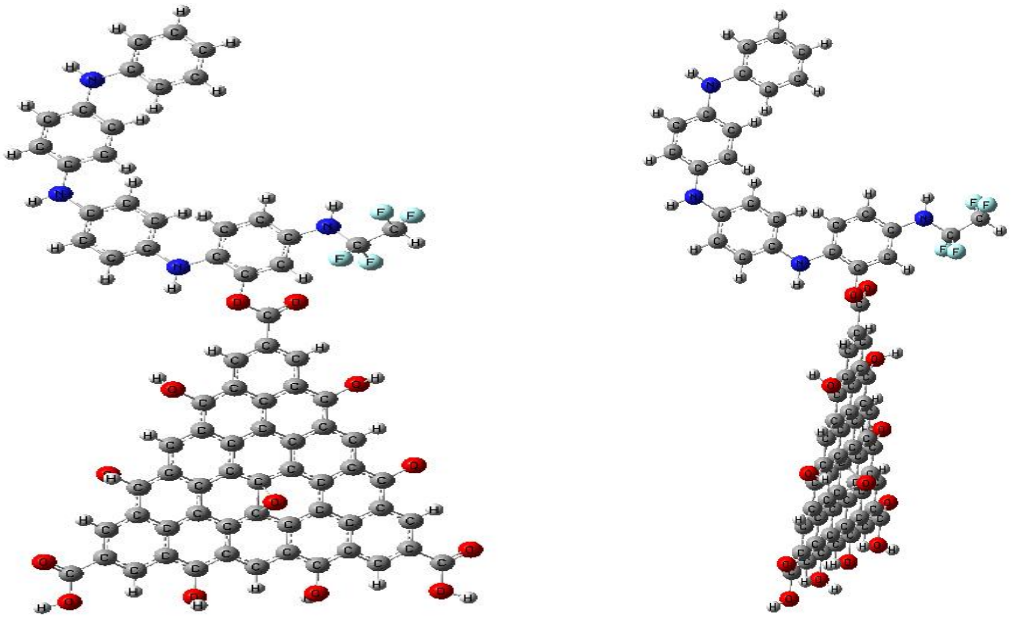

(a)

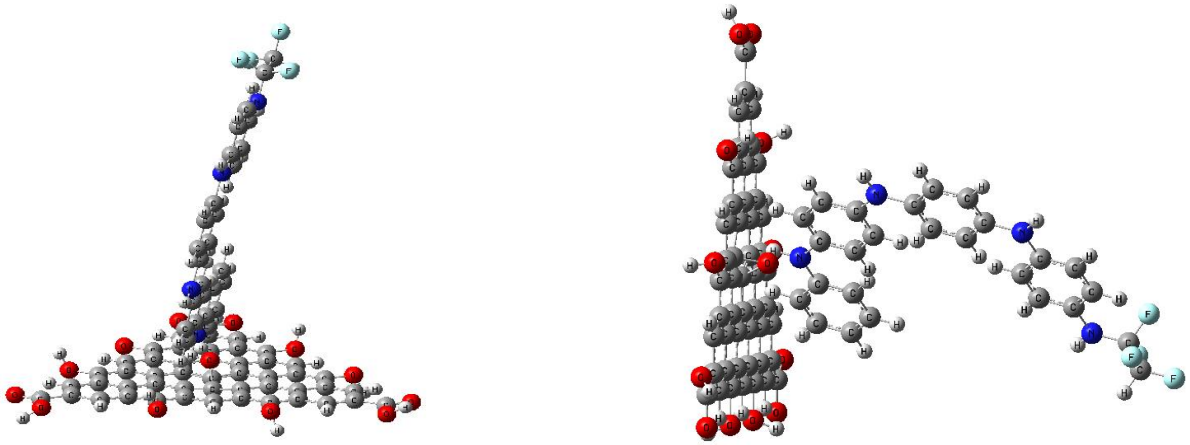

(b)

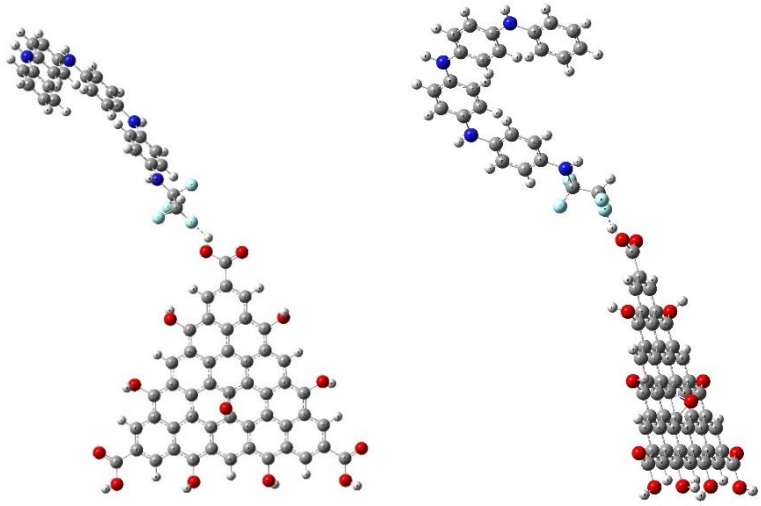

(c)

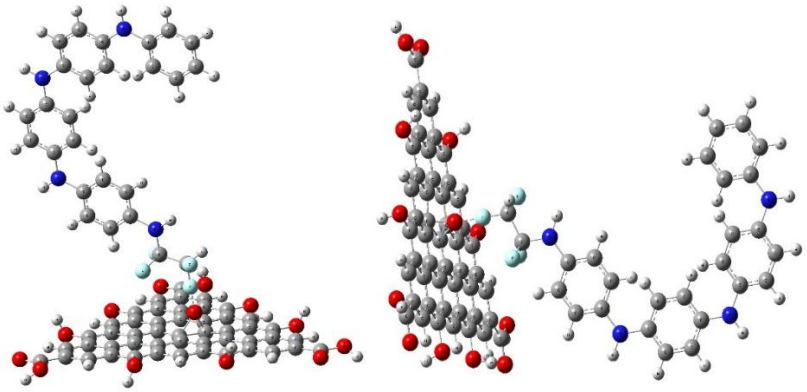

(d)

Figure 2. Model molecules representing (a) the top view of GO interacted with PANi / Teflon throughout the terminal and side view of GO interacted with PANi/Teflon throughout the terminal (b) the top view of GO interacted with PANi/Teflon throughout the middle and side view of GO interacted with PANi/Teflon throughout the middle (c) the top view of GO interacted with Teflon/PANi throughout the terminal and side view of GO interacted with Teflon/PANi throughout the terminal (d) the top view of GO interacted with Teflon/PANi throughout the middle and side view of GO interacted with Teflon/PANi throughout the middle.

Table 1 presents that the GO model molecule has a TDM of 2.584 Debye and bandgap energy of 0.345 eV. Meanwhile, the model molecule presenting PANi blended with Teflon has a TDM of 3.083 Debye and bandgap energy of 1.738 eV. Figure 3-a and c show the calculated bandgap energy of PANi/Teflon and GO, respectively.

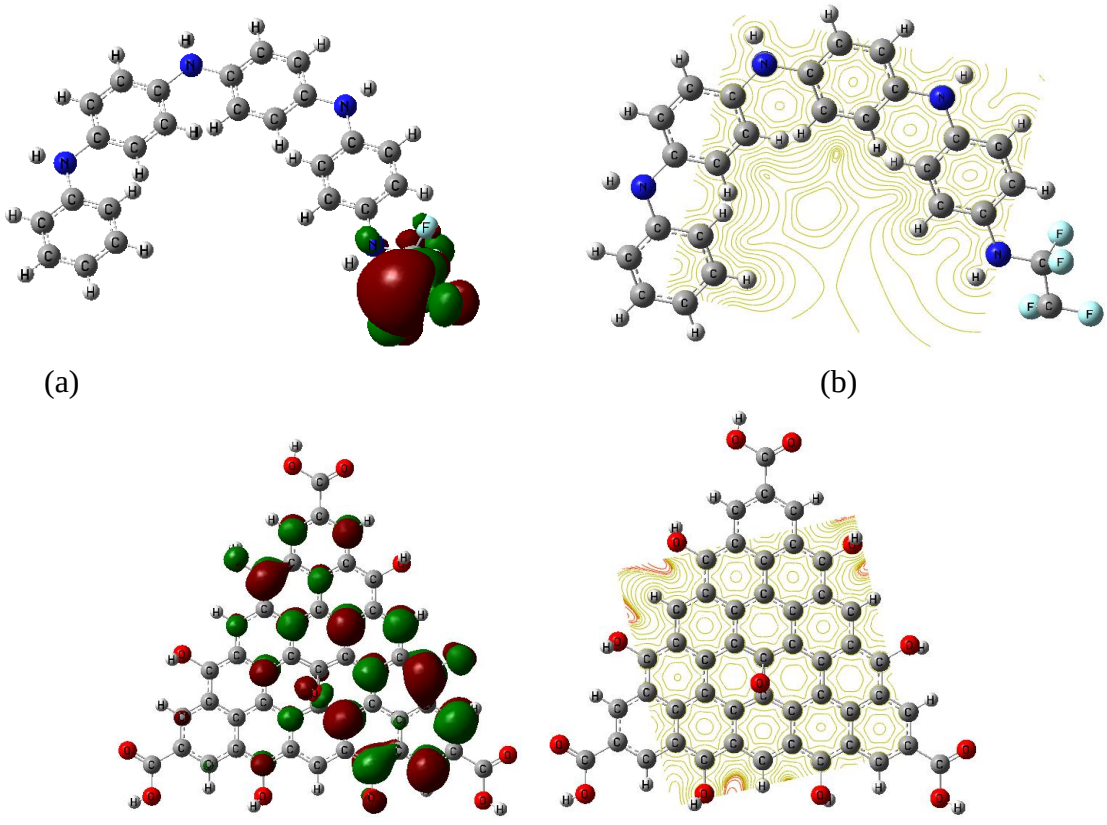

(a) (b)

(c) (d)

Figure 3. (a) The distribution of HOMO-LUMO bandgap energy of PANi/Teflon; (b) MESP as a contour of PANi/Teflon; (c) The distribution of HOMO-LUMO bandgap energy of GO and (d) MESP as a contour of GO

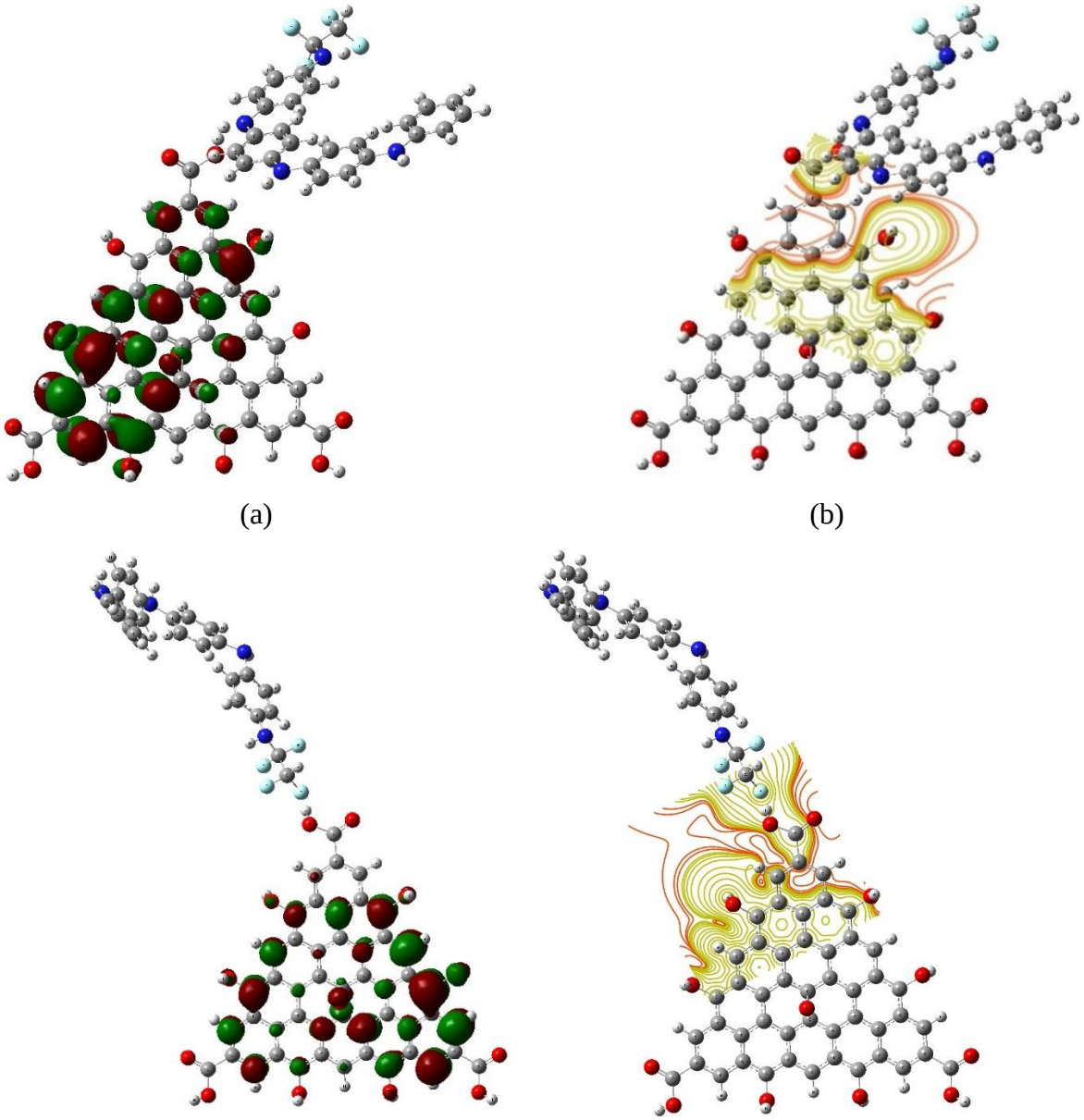

(a) (b)

(c) (d)

Figure 4. (a) The distribution of HOMO-LUMO band gap energy (b) MESP of GO interacted with PANi/Teflon throughout the terminal, (c) The distribution of HOMO-LUMO band gap energy (d) MESP of GO interacted with Teflon/PANi throughout the terminal.

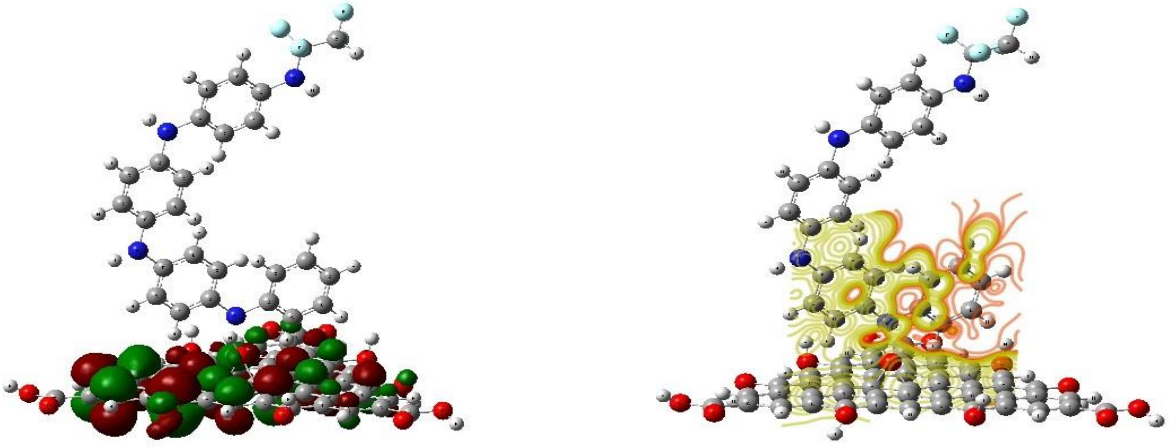

(a) (b)

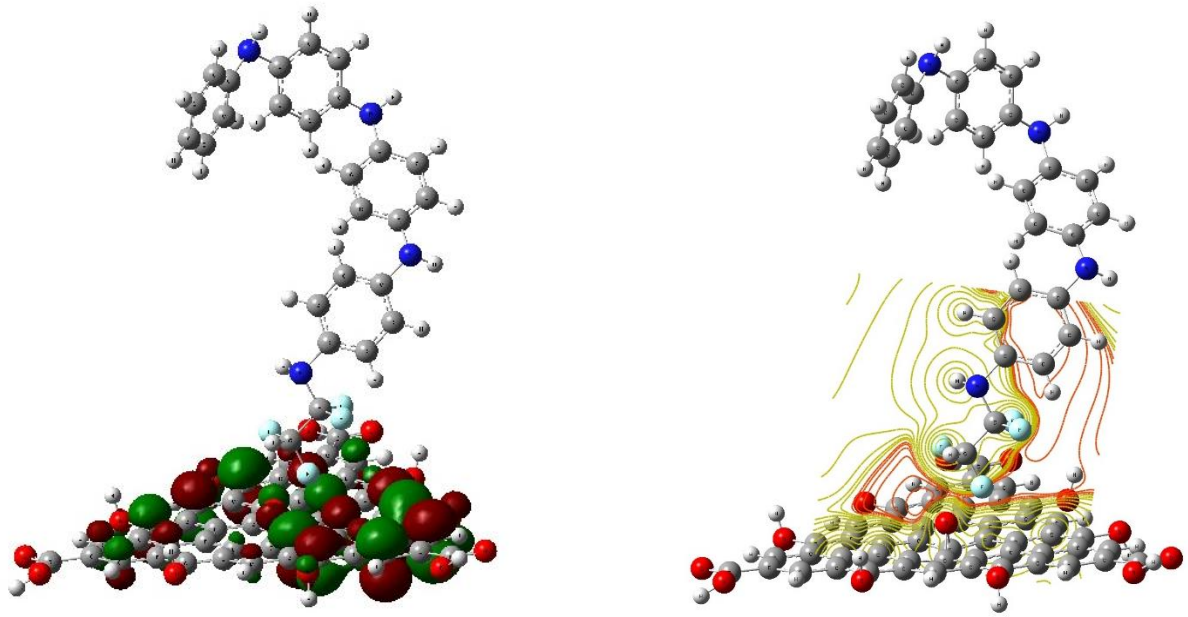

(c) (d)

Figure 5. (a) The distribution of HOMO-LUMO band gap energy (b) MESP of GO interacted with PANi/Teflon throughout the middle, (c) The distribution of HOMO-LUMO band gap energy (b) MESP of GO interacted with Teflon/PANi throughout the middle.

Figures 4-a and c and figure 5-a and c presents the HOMO-LUMO bandgap energy of GO interacted with PANi/Teflon from PANi once and from Teflon once throughout the terminal and middle of GO respectively. The effect of interaction is observed clearly from the changes that occurred in the TDM and bandgap energy values (see table 1). From the table, TDM of GO-Term (PANi/Teflon) and GO-Mid (PANi/Teflon) becomes 5.361 and 4.208 Debye while; their bandgap energy becomes 0.347 and 0.270 eV respectively. Also, TDM of GO-Term (Teflon/ PANi) and GO-Mid (Teflon/PANi) changed to 5.839and 1.436 Debye while their bandgap energy changed to 0.268 and 0.301 eV respectively. From the obtained results, it is clear that the TDM and bandgap energy value of GO depends strongly on the interaction position with the studied polymers and also on the modification occurs in the GO chemical structure. Where the energy gap becomes minor due to interaction throughout the middle O atom by PANI and when GO interacted with composite through Teflon from the terminal as 0.270 and 0.268 eV. The reason for this decrease of the bandgap energy of GO/PANi/Teflon model molecule is the presence of lone pairs of electrons provided by this group of atoms. Also, the results obtained confirmed that the interaction of GO with the blended PANi/Teflon occurs mainly via the middle O atom or the terminal when GO interacted with polymer through Teflon [39-40].

3.3. Molecular electrostatic potential (MESP).

The stability of the surface of GO, PANi/Teflon, and GO/PANi/Teflon structures are described by studying their MESP. The MESP describes the molecular reactivity by mapping the active sites in the studied structures (electrophilic and nucleophilic attack). These maps describe the distribution of electronic charges within the studied GO, PANi/Teflon, and GO/PANi/Teflon structures throughout colors. The different colors refer to differently charged regions. If these regions are very reached with electrons, i.e., highly electro-negative regions, the regions appeared red. Meanwhile, the regions which are neutral appear yellow, and those

with high positivity appear blue. This color mapping ongoing from negative to positive regions follows the sequence: red< orange < yellow < green < blue as described before [32-33].

Figure 3-b and figure 3-d show the calculated MESP as a contour for both PANi/Teflon and GO, respectively. The figures showed that the reactivity of GO is so small, and there are electronic charges only around some sites of the structure. At the same time, the calculated MESP of PANi/Teflon confirms the calculated results of TDM and bandgap energy where the structure is nearly neutral. Figure 4-b and figure 5-b show the calculated MESP as a contour for GO interacted with PANi/Teflon throughout the terminal and the middle, respectively. As shown in figures, the intensity of the red color increased due to the interaction of GO with the supposed structure of PANi/Teflon. Due to this interaction, the electronegativity of GO and the blended PANi/Teflon increased, and the reactivity enhanced greatly. These changes in the distribution of charges within the PANi/Teflon structure upon interaction with GO confirmed the suitability of GO/PANi/Teflon model for many applications such as energy storage materials, sensors, and drug delivery systems.

4. Conclusions

The electronic properties and structure stability of GO, PANi/Teflon, and GO/PANi/Teflon are studied using DFT. All the studied structures are optimized at B3LYB method using a 6-31g(d,p) basis set. In this study, GO is connected to the polymer via the O atom in the middle of GO structure. TDM for the studied structures are calculated and found to be increased as GO interacted with PANi/Teflon and reached to 5.361 and 4.208 Debye for GO-Term (PANi/Teflon) and GO- Mid (PANi/Teflon) respectively. Also, the bandgap energy for studied structures are calculated and found to be decreased to 0.347 and 0.270 eV for GO-Term (PANi/Teflon) and GO- Mid (PANi/Teflon), respectively. Also, TDM increased, and the bandgap energy decreased by changing the interaction position. Based on the obtained results, it is concluded that both TDM and bandgap energy depends on (a) attached group of polymer blend and (b) the position of interaction. MESP was studied as well for all the studied structures. All calculations confirmed that the reactivity of the studied structures increased due to the interaction of the polymer blend with GO. Additionally, the results confirmed that the most probable interaction between GO and the blended PANi/Teflon is that it proceeds through the O atom. The obtained results of TDM, bandgap energy, and MESP confirmed that the proposed structure of GO/PANi/Teflon could be used in the fabrication of electrochemical devices.

Funding

This research received no external funding.

Acknowledgments

This research has no acknowledgment.

Conflicts of Interest

The authors declare no conflict of interest.

References

1. Wang, G.; Zhang, L.; Zhang J. A review of electrode materials for electrochemical supercapacitors. *Chemical Society Reviews* **2012** *41*, 797-828, https://doi.org/10.1039/C1CS15060J.
2. Mi, H.; Zhou, J.; Zhao, Z.; Yu, C.; Wang, X.; Qiu J. Block copolymer–guided fabrication of shuttle–like polyanilinenanoflowers with radiated whiskers for application in supercapacitors. *RSC Advances* **2015,** *5*, 1016-1023, https://doi.org/10.1039/C4RA10273H.
3. Chen, W.; Rakhi, R.B.; Alshareef, H.N. Facile synthesis of polyaniline nanotubes using reactive oxide templates for high energy density pseudocapacitors. *Journal of Materials Chemistry A* **2013**, *1*, 3315-3324, https://doi.org/10.1039/C3TA00499F.
4. Wang, L.; Ye, Y.; Lu, X.; Wen, Z.; Li, Z.; Hou, H.; Song, Y. Hierarchical Nanocomposites of Polyaniline Nanowire Arrays on Reduced Graphene Oxide Sheets for Supercapacitors. *Scientific Reports* **2013,** *3*, https://doi.org/10.1038/srep03568.
5. Wang, L.; Lu, X.; Lei, S.; Song Y. Graphene-based polyanilinenanocomposites: preparation, properties and applications. *Journal of Materials Chemistry A* **2014,** *2*, 4491-4509,https://doi.org/10.1039/C3TA13462H.
6. Li, Y.; Zhao, X.; Xu, Q.; Zhang, Q.; Chen, D. Facile Preparation and Enhanced Capacitance of the Polyaniline/ Sodium Alginate Nanofiber Network for Supercapacitors. *Langmuir* **2011,** *27*, 6458-6463, https://doi.org/10.1021/la2003063.
7. Wang, X.; Deng, J.; Duan, X.; Liu, D.; Guo, J.; Liu, P. Crosslinked polyaniline nanorods with improved electrochemical performance as electrode material for supercapacitors. *Journal of Materials Chemistry A* **2014**, *2*, 12323-12329, https://doi.org/10.1039/C4TA02231A.
8. Xie, Y.; Liu, Y.; Zhao, Y.; Tsang, Y.H.; Lau, S.P.; Huang, H.; Chai, Y. Stretchable all-solid-state supercapacitor with wavy shaped polyaniline/graphene electrode. *Journal of Materials Chemistry A* **2014**, *2*, 9142-9149, https://doi.org/10.1039/C4TA00734D.
9. Hu, N.; Zhang, L.; Yang, C.; Zhao, J.; Yang, Z.; Wei, H.; Liao, H.; Feng, Z.; Fisher, A.; Zhang, Y.; Xu, Z.J. Three-dimensional skeleton networks of graphene wrapped polyaniline nanofibers: an excellent structure for high-performance flexible solid-state supercapacitors. *Scientific Reports* **2016**, *6*, https://doi.org/10.1038/srep19777.
10. Guo, F.; Mi, H.; Zhou, J.; Zhao, Z.; Qiu, J. Hybrid pseudocapacitor materials from polyaniline@multi-walled carbon nanotube with ultrafine nanofiber-assembled network shell. *Carbon* **2015**, *95*, 323-329, https://doi.org/10.1016/j.carbon.2015.08.052.
11. Yang, M.; Cheng, B.; Song, H.; Chen, X. Preparation and electrochemical performance of polyaniline-based carbon nanotubes as electrode material for supercapacitor. *Electrochimica Acta* **2010**, *55*, 7021-7027, https://doi.org/10.1016/j.electacta.2010.06.077.
12. Fan, H.; Wang, H.; Zhao, N.; Zhang, X.; Xu, J. Hierarchical nanocomposite of polyaniline nanorods grown on the surface of carbon nanotubes for high-performance supercapacitor electrode. *Journal of Materials Chemistry* **2012**, *22*, 2774-2780, https://doi.org/10.1039/C1JM14311E.
13. Kumar, R.; Joanni, E.; Singh, R.K.; Singh, D.P.; Moshkalev, S.A. Recent advances in the synthesis and modification of carbon-based 2D materials for application in energy conversion and storage. *Progress in Energy and Combustion Science* **2018**, *67*, 115-157, https://doi.org/10.1016/j.pecs.2018.03.001.
14. Kumar, R.; Oh, J.-H.; Kim, H.-J.; Jung, J.-H.; Jung, C.-H.; Hong, W.G.; Kim, H.-J.; Park, J.-Y.; Oh, I.-K. Nanohole-Structured and Palladium-Embedded 3D Porous Graphene for Ultrahigh Hydrogen Storage and CO Oxidation Multifunctionalities. *ACS Nano* **2015**, *9*, 7343-7351, https://doi.org/10.1021/acsnano.5b02337.
15. El-Khodary, S.A.; El-Enany, G.M.; El-Okr, M.; Ibrahim, M. Preparation and Characterization of Microwave Reduced Graphite Oxide for High-Performance Supercapacitors. *Electrochimica Acta* **2014**, *150*, 269-278, http://dx.doi.org/10.1016/j.electacta.2014.10.134.
16. Hwang, J.Y.; El-Kady, M.F.; Li, M.; Lin, C.W.; Kowal, M.; Han, X.; Kaner, R.B. Boosting the capacitance and voltage of aqueous supercapacitors via redox charge contribution from both electrode and electrolyte. *Nano Today* **2017**, *15*, 15-25, https://doi.org/10.1016/j.nantod.2017.06.009.
17. Tiwari, S.K.; Mishra, R.K.; Ha, S.K.; Huczko, A. Evolution of Graphene Oxide and Graphene: From Imagination to Industrialization. *ChemNanoMat* **2018**, *4*, 598-620, https://doi.org/10.1002/cnma.201800089.
18. Hughes, Z.E.; Walsh, T.R. Computational chemistry for graphene-based energy applications: progress and challenges. *Nanoscale* **2015**, *7*, 6883-6908, https://doi.org/10.1039/C5NR00690B.
19. Kumar, R.; Singh, R.K.; Singh, D.P.; Joanni, E.; Yadav, R.M.; Moshkalev, S.A. Laser-assisted synthesis, reduction and micro-patterning of graphene: Recent progress and applications. *Coordination Chemistry Reviews* **2017**, *342*, 34-79, https://doi.org/10.1016/j.ccr.2017.03.021.
20. Ates, M.; Caliskan, S.; Özten, E. Supercapacitor study of reduced graphene oxide/Zn nanoparticle/polycarbazole electrode active materials and equivalent circuit models. *Journal of Solid State Electrochemistry* **2018**, *22*, 3261-3271, https://doi.org/10.1007/s10008-018-4039-3.

21. Li, H.; Su, Q.; Kang, J.; Feng, H.; Huang, P.; Feng, M.; Huang, M.; Du, G. Fabrication of MoS_2@SnO_2-SnS_2 composites and their applications as anodes for lithium ion batteries. *Materials Research Bulletin* **2018**, *108*, 106-112, https://doi.org/10.1016/j.materresbull.2018.08.042.
22. Park, S.; Lee, K.-S.; Bozoklu, G.; Cai, W.; Nguyen, S.T.; Ruoff, R.S. Graphene Oxide Papers Modified by Divalent Ions—Enhancing Mechanical Properties via Chemical Cross-Linking. *ACS Nano* **2008**, *2*, 572-578, https://doi.org/10.1021/nn700349a.
23. Aghazadeh, M. One-step electrophoretic/electrochemical synthesis of reduced graphene oxide/manganese oxide (RGO-Mn_3O_4) nanocomposite and study of its capacitive performance. *Analytical and Bioanalytical Electrochemistry* **2018**, *10*, 961-973.
24. Alghunaim, N.S.; El-Khodary, S.A.; Ibrahim, M.; El-Enany, G.M. Spectroscopic analyses of iron doped protonated polyaniline/graphene oxide system. *Spectrochimica Acta Part A* **2019**, *216*, 349-358, https://doi.org/10.1016/j.saa.2019.03.053.
25. Bayoumy, A.M.; Refaat, A.; Yahia, I.S.; Zahran, H.Y.; Elhaes, H.; Ibrahim, M.A.; Shkir, M. Functionalization of graphene quantum dots (GQDs) with chitosan biopolymer for biophysical applications. *Optical and Quantum Electronics* **2019**, *52*, 1-14. https://doi.org/10.1007/s11082-019-2134-z.
26. Grenni, P.; Barra Caracciolo, A.; Mariani, L.; Cardoni, M.; Riccucci, C.; Elhaes, H.; Ibrahim, M.A. Effectiveness of a new green technology for metal removal from contaminated water. *Microchemical Journal* **2019**, *147*, 1010-1020, https://doi.org/10.1016/j.microc.2019.04.026.
27. Fahmy, A.; Khafagy, R.M.; Elhaes H.; Ibrahim M.A. Molecular Properties of Polyvinyl Alcohol/Sodium Alginate Composite. *Biointerface Research in Applied Chemistry* **2020,** *10*, 4734-4739, https://doi.org/10.33263/BRIAC101.734739.
28. Refaat, A.; Ibrahim, M.A.; Elhaes, H.; Badry, R.; Ezzat, H.; Yahia, I.S.; Zahran, H.Y.; Shkir, M. Geometrical, vibrational and physical properties of polyvinyl chloride nanocomposites: Molecular modeling approach. *Journal of Theoretical and Computational Chemistry* **2019**, *18*, https://doi.org/10.1142/S0219633619500378.
29. Ezzat, H.A.; Hegazy, M.A.; Nada N.A.; Ibrahim M.A. Effect of Nano Metal Oxides on the Electronic Properties of Cellulose, Chitosan and Sodium Alginate. *Biointerface Research in Applied Chemistry* **2019,** *9*, 4143-4149, https://doi.org/10.33263/BRIAC94.143149.
30. Ibrahim, M.; Elhaes, H. Computational Spectroscopic Study of Copper, Cadmium, Lead and Zinc Interactions in the Environment. *International Journal of Environment and Pollution* **2005**, *23*, 417-424, https://doi.org/10.1504/IJEP.2005.007604.
31. Ibrahim, M.; Mahmoud, A.A. Computational Notes on the Reactivity of Some Functional Groups. *Journal of Computational and Theoretical Nanoscience* **2009**, *6*, 1523-1526, https://doi.org/10.1166/jctn.2009.1205.
32. Politzer, P.; Laurence, P.R.; Jayasuriya, K. Molecular electrostatic potentials: an effective tool for the elucidation of biochemical phenomena. *Environmental Health Perspectives* **1985**, *61*, 191-202, https://doi.org/10.1289/ehp.8561191.
33. ahin, Z.S.; Şenöz, H.; Tezcan, H.; Büyükgüngör, O. Synthesis, spectral analysis, structural elucidation and quantum chemical studies of (E)-methyl-4-[(2-phenylhydrazono)methyl]benzoate. *Spectrochimica Acta Part A* **2015**, *143*, 91-100, https://doi.org/10.1016/j.saa.2015.02.032.
34. Frisch, M.J. et. al. Gaussian09, revisions D. 01 and B. 01; Gaussian, Inc. *Wallingford, CT* **2010**.
35. Becke, A.D. Density-functional thermochemistry. III. The role of exact exchange. *The Journal of Chemical Physics* **1993**, *98*, 5648-5652, https://doi.org/10.1063/1.464913.
36. Lee, C.; Yang, W.; Parr, R.G. Development of the Colle-Salvetti correlation-energy formula into a functional of the electron density. *Physical Review B* **1988**, *37*, 785-789, https://doi.org/10.1103/PhysRevB.37.785.
37. Miehlich, B.; Savin, A.; Stoll, H.; Preuss, H. Results obtained with the correlation energy density functionals of becke and Lee, Yang and Parr. *Chemical Physics Letters* **1989**, *157*, 200-206, https://doi.org/10.1016/0009-2614(89)87234-3.
38. Abdelsalam, H.; Elhaes, H.; Ibrahim, M.A. Tuning electronic properties in graphene quantum dots by chemical functionalization: Density functional theory calculations. *Chemical Physics Letters* **2018**, *695*, 138-148, https://doi.org/10.1016/j.cplett.2018.02.015.Badry, R.; El-Khodary, S.; Elhaes, H.; Nada, N.; Ibrahim, M. On the molecular modeling analyses of sodium carboxymethyl cellulose treated with acetic acid. *Letters in Applied NanoBioScience* **2019**, *8*, 553-557, https://doi.org/10.33263/LIANBS 82.553557.
39. Ibrahim, A.; Elhaes, H.; Ibrahim, M. Computational notes on the electronic properties of carboxylic acid. *Letters in Applied NanoBioScience* **2020**, *9*, 1079-1082, https://doi.org/10.33263/LIANBS92.10791082.